Molecular Crystals and Liquid Crystals Science and Technology. Section A. Molecular Crystals and Liquid Crystals

Publication details, including instructions for authors and subscription information:
http://www.tandfonline.com/loi/gmcl19

# Infrared Microspectroscopic Investigation of the Diffusion of E7 into PiBMA

B. G. Wall [a] & J. L. Koenig [a]

[a] Macromolecular Science Department, Case Western Reserve University, Cleveland, OH, 44121

Version of record first published: 24 Sep 2006

To cite this article: B. G. Wall & J. L. Koenig (1999): Infrared Microspectroscopic Investigation of the Diffusion of E7 into PiBMA, Molecular Crystals and Liquid Crystals Science and Technology. Section A. Molecular Crystals and Liquid Crystals, 326:1, 101-112

To link to this article: http://dx.doi.org/10.1080/10587259908025408

*Mol. Cryst. Liq. Cryst.*, Vol. 326, pp. 101 - 112
Reprints available directly from the publisher
Photocopying permitted by license only





# Infrared Microspectroscopic Investigation of the Diffusion of E7 into PiBMA

B. G. WALL and J. L. KOENIG*

*Macromolecular Science Department, Case Western Reserve University, Cleveland, OH 44121*

*(Received 15 June 1998; In final form 30 July 1998)*

The components of a liquid crystal mixture (E7) have been shown to diffuse at different rates in Polymer Dispersed Liquid Crystals (PDLCs). It was observed in this work that liquid crystals of different molecular weights diffuse into poly(isobutyl methacrylate) (PiBMA) at different rates at a constant temperature. It was also determined that the components in a liquid crystal mixture diffuse into the polymer at different rates. The effect is quite small under normal conditions, so elevated temperatures, simplified diffusion boundaries and extended time scales were employed to magnify the diffusion separation effects for study. Although this work demonstrates that these components diffuse at different rates, the short phase separation times experienced during the generation of a PDLC are probably insufficient to promote this effect to the point where optical properties are adversely affected.

*Keywords:* Infrared Microspectroscopy; poly(isobutyl methacrylate); liquid crystal; E7; diffusion; contact method; mapping

## INTRODUCTION

Polymer Dispersed Liquid Crystals [1 - 3] (PDLCs) are liquid crystals (LCs) combined with polymers in various ways [4 - 9] to make attractive electro-optic devices [4 - 6]. In PDLCs, the polymer is the major-phase, continuous matrix while the liquid crystal is the minor phase, and takes the form of many tiny droplets evenly dispersed throughout the polymer. These systems scatter light when the alignment of the liquid crystals within the droplets are aligned independently from droplet to droplet. These systems transmit light

*Corresponding author. Tel.: (216) 368-4176, Fax: (216) 368-4171, e-mail: jlk6@po.cwru.edu

when the alignments of the liquid crystals in each droplet are in the same direction, along the direction of view. There are many parameters that need to be controlled in the production of these systems to achieve optimally viable systems [2, 10–12]. One of the major concerns is refractive index matching. In order for the PDLCs to transmit light when the liquid crystals are all aligned along the direction of view, the refractive index of the liquid crystal phase along the direction of transmission must closely match the refractive index of the polymer. Conversely, in order to get efficient scattering of light, the refractive index of the liquid crystal phase along the other optical axis must be as different as possible from the refractive index of the polymer. Liquid crystal mixtures are carefully designed to posses this quality for each polymer/liquid crystal system. The phase separation processes surrounding these systems have been studied in recent years [13–19] but the question of differential segregation, *i.e.*, the components of a liquid crystal mixture diffusing at different rates in the manufacture of PDLCs, has not been adequately addressed.



## APPROACH

Previous work has demonstrated the feasibility of using IR microscopy to study PDLCs. The foundation of this work is based on the ability to resolve the four liquid crystal components of E7 with Fourier transform, infrared (FTIR) microspectroscopy, taking advantage of the 10 μm spatial resolution and redundant aperturing of the infrared microscope [20, 21]. Figure 1 shows the nitrile band in the infrared spectrum of each component and of E7, the relative concentrations of each in E7, and their chemical structures. The nitrile bands are resolvable at a resolution of $2\,cm^{-1}$. CB and CT stand for cyanobiphenyl and cyanotriphenyl respectively. OCB indicates that there is an oxygen atom between the hydrocarbon tail and the biphenyl system. The numbers 5, 7 and 8 describe the number of carbons in the linear, hydrocarbon arm opposite the nitrile group on the appropriate phenyl system of these materials.

## EXPERIMENTAL

A glass, microscope slide was sprayed with an atomizer vessel containing five-micrometer-diameter glass spacer material using methanol as a carrier solvent. The slide was then placed onto a hot plate and heated at 80°C to

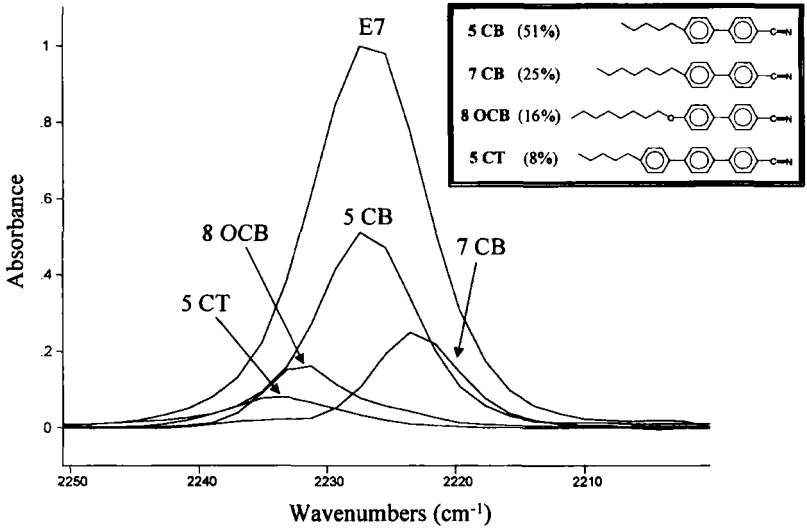


FIGURE 1 Nitrile bands and structures of E7 and its four components.

drive off the methanol and any water. A small amount of poly(isobutyl methacrylate) (PiBMA) was placed onto the glass slide. This was heated on a hot plate at 140°C until the translucent polymer solid softened and turned clear. A glass cover slip was then placed onto the polymer. Pressure was exerted from the top to level and spread the polymer, and to decrease the sample thickness as much as possible. The sample was then removed from the hot plate. Another glass slide was placed on top of the cover slip and two medium-size binder clips were clamped over the center of the polymer region. The second glass slide was used to prevent the cover slip from being broken under the force of the binder clips and to allow the entire polymer region to be compressed uniformly. This whole assembly was then placed into an oven set at 140°C and left overnight. At this temperature, and under the force of the binder clips, the polymer continued to spread unitl the sample thickness was defined by the five-micrometer glass spacers. This ensured a uniform, five-micrometer thick polymer film. The sample was removed from the oven after 24 hours and was allowed to cool. A clear polymer film was then evident inside the glass slide/cover slip cell. The polymer film was approximately circular and about one centimeter in diameter.

The contact method [16, 17, 22–26] was then employed to create the idealized phase boundary. The cell containing the polymer film was placed onto a hot plate at 60°C and was allowed to equilibrate. At this temperature, 5 CB and 7 CB are isotropic and 8 OCB is smectic. Each liquid crystal was

then introduced into the cell by placing a drop on the glass slide/cover slip interface on the side of the cell away from the polymer. The drop made contact with both substrates and made its way into the cell by capillary action. When the liquid crystal made first contact with the polymer film, time zero was established and the diffusion of the liquid crystal into the polymer began. Each of the liquid crystals 5 CB, 7 CB, and 8 OCB was diffused into PiBMA at 60°C. 5 CT was not used because it remains a solid at 60°C. It was presumed that the diffusion profile of this component could be obtained by spectral subtraction, by subtracting out the spectral contributions of the other liquid crystal components from the experimental data. Each component used was allowed to diffuse for five, ten and twenty minutes, each on fresh (nondiffused) samples. At the end of the time intervals, the cells were removed from the hot plate and quenched. Point by point spectral maps were then acquired to determine the extent and character of the diffusion region in each sample. The infrared beam was apertured. Along the direction of the map, the aperture was narrow (14 μm) to maximize the spatial resolution of the experiment. The perpendicular dimension of the aperture was kept large (293 μm) to allow for good signal throughput. Spatial resolution was further enhanced by acquiring data at 7 μm step intervals. This type of aperture enhancement was possible because of the linear diffusion boundary designed into the experiment and would not normally be possible in a traditional PDLC sample. The spectra from the diffusion regions were processed to reduce the spectral data to a component-specific, absorption matrix of the sample, showing the intensity of the nitrile band *versus* position in each sample, yielding spatially resolved absorption data. The absorption profile thus obtained for each sample was then subjected to data fitting techniques to determine the diffusion coefficient of each component. The diffusion regions were measured and the diffusion coefficients determined for each component. Then, the contact method was used again, but this time with E7 instead of E7's individual components. The spectra were processed as before adding the technique of spectra subtraction to elucidate the extent of segregation of the components of E7 in a real diffusion case.

It is necessary to define the experimental boundary conditions. It is considered that we are dealing with a one-dimensional diffusion condition dealing with small molecules diffusing into the polymer matrix. This is because the liquid crystal molecules are diffusing in one direction on the scale of the infrared probe. The initial experimental conditions are when $t$(time) = 0, then $C$(concentration) = $C_0$ (initial concentration). The boundary conditions are such that at $L$ (distance) = 0, $C = C_0$, and at $L = \infty$,

$C = 0$, *i.e.*, the liquid crystal has not diffused a large distance into the polymer on the time scale of the experiment. The experiment is done above the $T_g$ of the polymer. However, the polymer moves much more slowly than the liquid crystals so we define the polymer phase as stationary by setting the polymer boundary in each case to $L = 0$. We then consider this experimental diffusion versus time, neglecting any concentration dependence of the diffusion coefficient, $D$. Therefore, we apply Fick's Law of Diffusion [27].

$$\frac{\partial C}{\partial t} = D\frac{\partial^2 C}{\partial x^2} \tag{1}$$

When this differential equation is solved using the stated boundary conditions, the solution (Eq. (2)) is given below using the complimentary error function [28] (erfc).

$$\frac{C}{C_0} = \frac{1}{2}\text{erfc}\frac{L}{\sqrt{4Dt}} \tag{2}$$

This solution can be rearranged into a form that is easy to plot (Eq. (3)), and that allows for the direct determination of the diffusion coefficient, $D$.

$$y = \text{erfc}\left(\frac{x}{\sqrt{D}}\right) \tag{3}$$

In this arrangement (Eqs. (4), (5)),

$$y = \frac{2C}{C_0}, x = \frac{L}{2\sqrt{t}} \tag{4, 5}$$

Thus, knowing the absorption magnitude ($A = f(C)$) for each sampled diffusion distance ($L$) and the time ($t$) of each diffusion experiment, the diffusion coefficient ($D$) was calculated using the erfc curve fitting function in a spread sheet program.

Data obtained from the Spectra-Tech Inc., infrared microscope (IRμs), was collected from 4000 to 2100 $cm^{-1}$, at a resolution of 2 $cm^{-1}$. Using glass as the substrate material prevented data acquisition below this range, but still allowed the nitrile bands at $\sim 2228\,cm^{-1}$ to be used for data analysis. 64 co-added spectra were collected for each data spectrum to reduce noise to a reasonable level. The IRμs possesses traditional FTIR technology, which uses constant mirror velocity interferometry and a mercury cadmium telluride (MCT) detector. Infrared data and optical micrographs collected on the IRμs were processed with OMNIC and Atlμs software from Nicolet.

## RESULTS

An optical micrograph and the nitrile band profile from the diffusion region for 7 CB diffused into PiBMA is shown as Figure 2. Figure 3 shows a nitrile band profile covering the full wavenumber range illustrating the PiBMA and LC regions and the diffusion region as well as the points where the concentration of polymer and liquid crystal were determined to be zero. The distance between the two zero points was calculated in μm from the known acquisition parameters in each experiment. These diffusion distances were used in calculating the diffusion coefficients. The liquid crystal region shows a rise above the diffusion zero point where the system is phase separated. The absorbance value then decreases as the liquid crystal well thins and eventually is not in complete contact with both substrates. The objects in the figure that appear similar to bubbles on the PiBMA side of the diffusion region are regions where the system has phase separated. The circular objects on the 7 CB side of the figure are regions of phase separation where reverse morphology is evident. Normal PDLC morphology has the liquid crystal contained in tiny phase separated droplets. Reverse morphology is obtained when the concentration of polymer is so low that the polymer takes the form of the tiny droplets.

The concentration profiles of the nitrile bands were processed in the following way to determine diffusion coefficients ($D$). Sample position across the diffusion region and concentration (absorbance) data were normalized

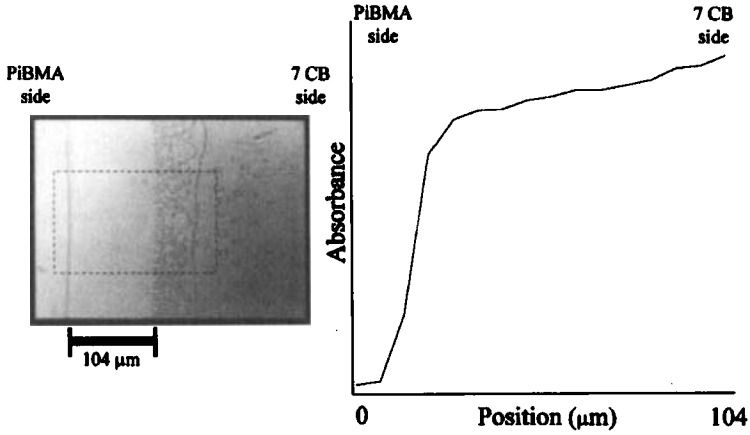


FIGURE 2 Optical micrograph and 2228 $cm^{-1}$ profile of 7 CB in PiBMA. The dashed-line box indicates the sampled region. (See Color Plate III).

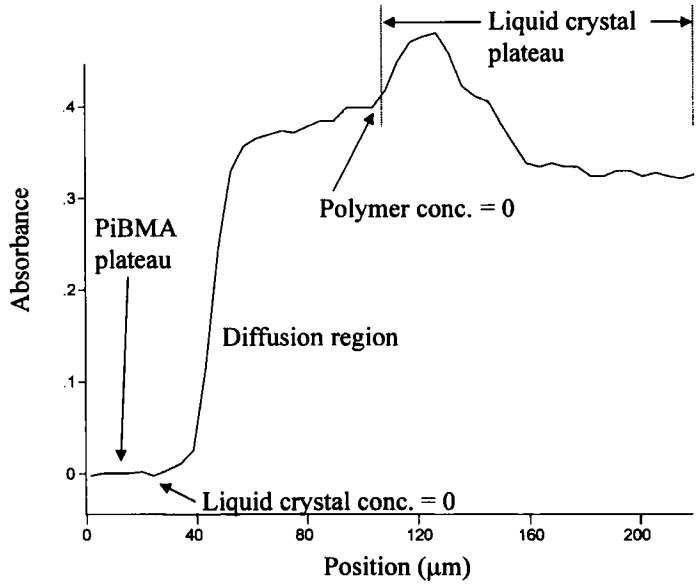


FIGURE 3 Nitrile band profile showing polymer and liquid crystal plateaus, and the diffusion region concentration gradient.

from zero to one for each sample. The normalized position values were divided by the appropriate time intervals (Eq. (5)). An estimate of the diffusion coefficient was then inserted into the erfc equation using the normalized concentration and position data (Eq. (3)). The data were plotted graphically using Microsoft Excel. Readjustment of the estimated diffusion coefficient was then made until the erfc function fit all of the data within +/− 10%. After the best fit diffusion coefficients were calculated, the components were ranked 5 CB, 7 CB, 8 OCB, with 5 CB having the largest and 8 OCB having the smallest diffusion coefficient. Figure 4 shows a summary of the segregation predictions based on molecular weight considerations and preliminary experimental findings with the individual components.

From these predictions and investigations of the individual components of E7, it can be seen that all of the results are internally consistent. That is, 5 CB is the smallest molecule, has the widest diffusion region, and has the largest diffusion coefficient. Assuming the behavior of the components in E7 will not change when starting as a mixture, 5 CB will be more highly concentrated at the moving wave front of the separating liquid crystal phase, and the other components will lag behind in the order 7 CB, 8 OCB. It was assumed that 5 CT would diffuse the slowest based on the precedent established by the other components.

| Component | Concentration (%) | Width of 20-minute Diffusion Region (μm) | Calculated Diffusion Coefficient (μm2/min) | Relative Diffusion Rate |
|---|---|---|---|---|
| 5 CB | 51 | 70 | 300 | fastest |
| 7 CB | 25 | 56 | 280 | moderate |
| 8 OCB | 16 | 36 | 25 | slow |
| 5 CT | 8 | ---- | ---- | (slowest) |

FIGURE 4 Summary of data for components of E7 diffusing into PiBMA at 60°C.



For the data processing of the E7 experimental spectra, it was assumed that 5 CB would be the liquid crystal component on the leading edge of the diffusion wave front. The nitrile band at this point in the diffusion region was normalized to the nitrile band from the spectrum of pure 5 CB. The nitrile band from the spectrum of 5 CB was then subtracted from the nitrile band of the experimental spectrum. The subtraction result yielded a flat line indicating that the nitrile band from the spectrum at the leading edge of the diffusion wave front was 5 CB. Every point of the diffusion region was then processed in this way by comparing the nitrile bands to that of pure 5 CB. For a certain distance extending into the diffusion region, subtracting the nitrile band of 5 CB from each experimental data point yielded straight lines also. Eventually, subtracting the nitrile band of 5 CB did not yield a straight line but contained a residual lobe at $2222\,cm^{-1}$ corresponding to the nitrile band for 7 CB. The subtraction spectra resulting from subtracting 5 CB from the diffusion region spectra (Fig. 5) show the build up in intensity of the 7 CB band. The numbers (μm) marked on the figure indicate the relative distances of penetration into the diffusion region of the sample.

This data processing routine is repeated over the entire diffusion region until successive spectral subtractions expose the remaining components of E7 at different distances away from the diffusion front. Subtracting the nitrile bands of 5 CB and 7 CB results in a band appearing at $2232\,cm^{-1}$ corresponding to the nitrile band of 8 OCB. Subtracting 5 CB, 7 CB and 8 OCB from the next few data points results in a residual band at $2233\,cm^{-1}$ corresponding to the nitrile band of 5 CT. The subtraction spectra resulting from subtracting 5 CB from the diffusion region spectra (Fig. 6) show the build up in intensity of the 8 OCB and 5 CT bands as indicated.

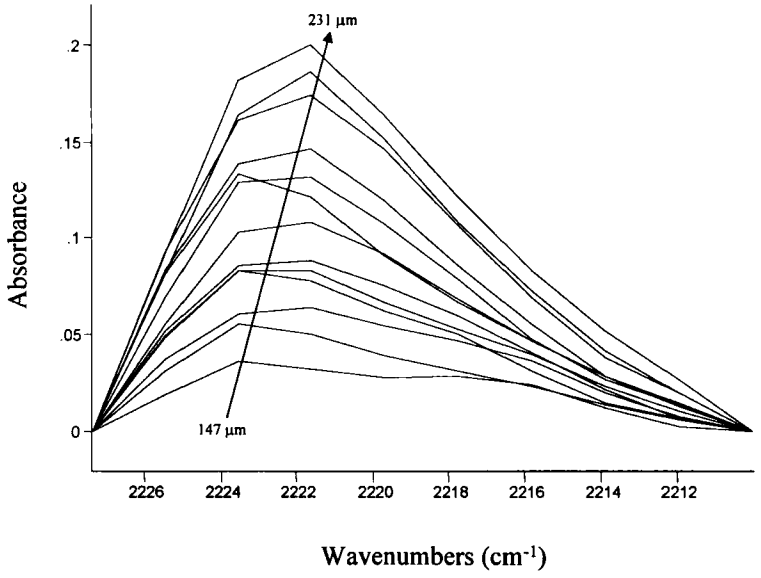


FIGURE 5 Subtraction results showing the appearance and increase of the 7 CB band.

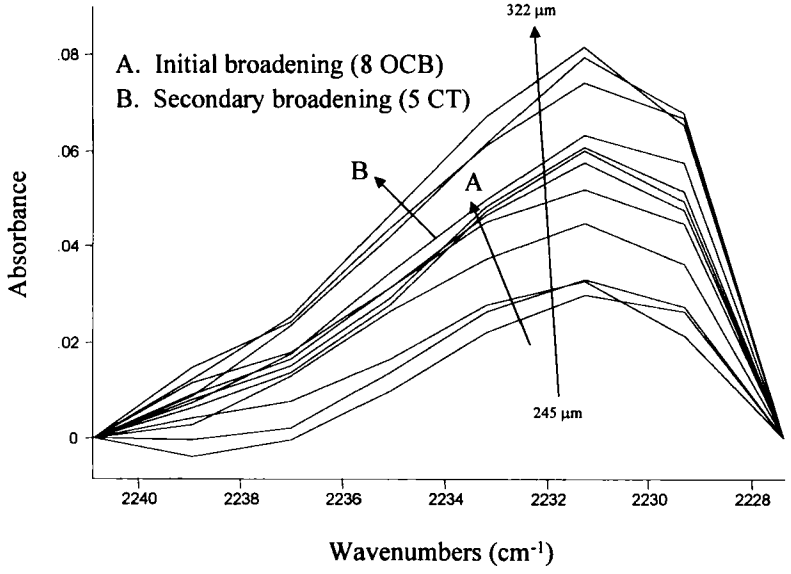


FIGURE 6 Subtraction results showing the appearance and increase of the 8 OCB and 5 CT bands.

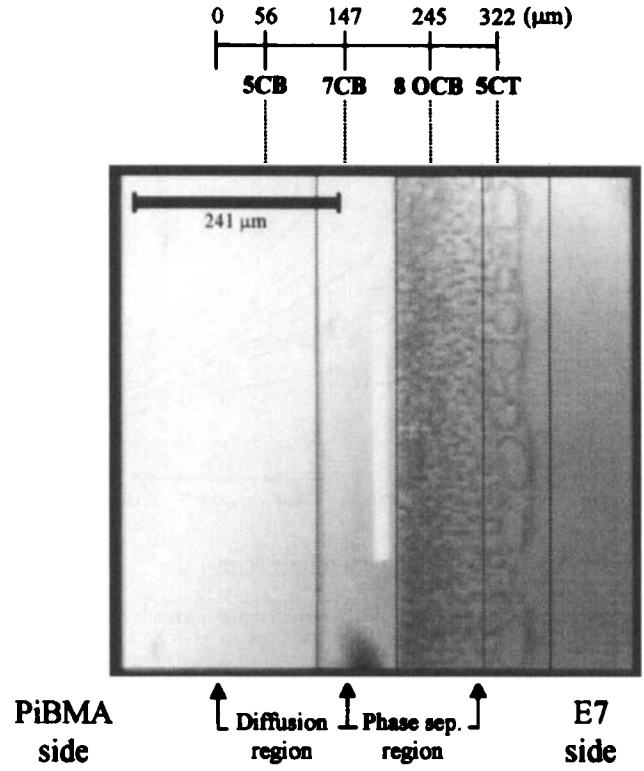


FIGURE 7 Optical micrograph of E7 diffused into PiBMA showing spectroscopically determined wave fronts of components. (See Color Plate IV).

Figure 7 shows optically the positions were the diffusion fronts of the components of E7 appear as well as the order of appearance. Each component appears at a different diffusion distance into the polymer. Because the diffusion was run at a temperature close to the $T_g$ of the polymer ($T_g$ = 55°C), diffusion of the liquid crystalline components is somewhat restricted. However, this data demonstrates that the components not only diffuse at different rates, but do so in the order predicted based on molecular weight and individual component diffusion parameters.

## CONCLUSIONS

It has been shown by this work that under designed experimental conditions the four components of E7 diffuse at different rates in PiBMA. Each

component has been shown to possess its own wave front within the diffusion region. The position of each component's wave front can be determined by FTIR at sufficiently high resolution. Further, it is important to observe that the components of E7 diffuse independently of each other in the polymer. More work needs to be done to ascertain the effect that differential diffusion may have in the generation of PDLCs. The improvements made on these systems have been dramatic in recent years. Because of these major improvements, smaller issues may now surface. If refractive index matching is being affected by this differential diffusion process, taking the effect into account during the engineering stage of PDLC development may result in further improvements in the optical quality and performance of PDLC devices. To quantify the impact of differential diffusion on display devices the magnitude of the effect under real conditions will have to be determined. When this is done, the challenge of considering the opposing effects of diffusion rate (small molecules move the fastest) *versus* immiscibility (small molecules are likely more miscible) may need to be addressed. These ideas are the subjects of future work in this area.



## References


[1] J. W. Doane, A. Golemme, J. L. West, J. B. Whitehead and B.-G. Wu, *Mol. Cryst. Liq. Cryst.*, **165**, 511 (1988).
[2] J. L. West, "Polymer Dispersed Liquid Crystals', *Advances in Liquid Crystal Polymer*, R. A. Weiss and C. K. Ober, Eds., ACS Symposium series, **435**, 475 (1990).
[3] J. W. Doane, "Polymer dispersed Liquid Crystal Displays', *Liquid Crystals Application and Uses*, B. Bahadur, Ed., World Scientific Press, London, **1**, 57 (1990).
[4] J. W. Doane, N. A. Vaz, B. G. Wu and S. Zumer, *Appl. Phys. Lett.*, **48**, 269 (1986).
[5] N. A. Vaz, G. W. Smith and G. P. Montgomery Jr., *Mol. Cryst. Liq. Cryst.*, **146**, 17 (1987).
[6] J. L. West, *Mol. Cryst. Liq. Cryst.*, **157**, 427 (1988).
[7] G. W. Smith, *Mol. Cryst. Liq. Cryst.*, **180B**, 210 (1990).
[8] G. W. Smith and N. A. Vaz, *Liq. Cryst.*, **3**, 543 (1988).
[9] G. W. Smith, *Mol. Cryst. Liq. Cryst.*, **196**, 89 (1991).
[10] P. S. Drzaic, "Liquid Crystal Displays and Applications", *Proc. SPIE*, **1257**, 29 (1990).
[11] G. Crawford, R. Ondris-Crawford and J. W. Doane, "Liquid Crystal Devices and Materials", *Proc. SPIE*, **1455**, 2 (1991).
[12] H. S. Kitzerow, *Liquid Crystals*, **16**, 1 (1994).
[13] J. Y. Kim and P. Palffy-Muhoray, *Mol. Cryst. Liq. Cryst.*, **203**, 95 (1991).
[14] Y. Hirai, S. Niiyama, H. Kumai and T. Gunjima, *SPIE*, **1257**, 2 (1990).
[15] C. A. McFarland, J. L. Koenig and J. L. West, *Appl. Spectrosco.*, **47**(5), 598 (1993).
[16] S. R. Challa, S.-Q. Wang and J. L. Koenig, *Appl. Spectrosco.*, **49**(3), 267 (1995).
[17] S. R. Challa, S.-Q. Wang and J. L. Koenig, *Appl. Spectrosco.*, **50**(11), 1339 (1996).
[18] S. R. Challa, S.-Q. Wang and J. L. Koenig, *Appl. Spectrosco.*, **51**(3), 297 (1997).
[19] S. R. Challa, S.-Q. Wang and J. L. Koenig, *Appl. Spectrosco.*, **51**(1), 10 (1997).
[20] R. G. Messerschmidt and M. A. Harthcock, *Infrared Micro-spectroscopy Theory and Applications*, Marcel Dekker, New York (1988).
[21] K. Krishnan and S. L. Hill, *Practical Fourier Transform Infrared Spectroscopy Industrial and Laboratory Chemical Analysis*, J. R. Ferraro and K. Krishnan, Eds., Academic Press, London p.103 (1990).

[22] G. Sigaud, M. F. Achard, F. Hardouin, M. Mauzac, H. Richard and H. Gasparoux, *Macromolecules*, **20**, 578 (1987).
[23] G. Sigaud, M. F. Achard, F. Hardouin and H. Gasparoux, *Mol. Cryst. Liq. Cryst.*, **155**, 443 (1988).
[24] G. Sigaud, M. F. Achard, F. Hardouin, C. Coulon, H. Richard and M. Mauzac, *Macromolecules*, **23**, 5020 (1990).
[25] F.-L. Chen and A. M. Jamieson, *Liq. Cryst.*, **15**, 171 (1993).
[26] C. M. Snively and J. L. Koenig, *Macromolecules*, **31**, 11, 3753 (1998).
[27] J. Crank, *The Mathematics of Diffusion*, Oxford University Press, London, p. 2 (1967).
[28] J. J. Sahlin and N. A. Peppas, *Macromolecules*, **29**, 7124 (1996).